

SYNTHESIS AND CHARACTERIZATION OF ZINC OXIDE NANOPARTICLES BY SOL-GEL PROCESS

*A Dissertation submitted in partial fulfillment of
the requirements for the degree of*



Master of Science

in

PHYSICS

By

SURYA PRAKASH GHOSH

ROLL NO-410PH2126

Under the supervision of

Prof. Seemanchal.Panigrahi

National Institute of Technology, Rourkela

Rourkela-769008, Orissa, India

May-2012

Synthesis and Characterization of Zinc Oxide Nanoparticles by Sol-Gel Process

*A Dissertation submitted in partial fulfillment of
the requirements for the degree of*



Master of Science

in

PHYSICS

By

SURYA PRAKASH GHOSH

ROLL No: 410PH2126

Under the supervision of

Prof. Seemanchal.Panigrahi

National Institute of Technology, Rourkela

Rourkela-769008, Orissa, India

May-2012

Department of Physics



National Institute of Technology, Rourkela

Rourkela-769008, Orissa, India

CERTIFICATE

This is to certify that, the work in the report entitled “**Synthesis and Characterization of Zinc Oxide Nanoparticles by Sol-Gel Process**” by **Mr Surya Prakash Ghosh**, in partial fulfilment of Master of Science degree in **PHYSICS** at the National Institute of Technology, Rourkela(Deemed University); is an authentic work carried out by him under my supervision and guidance. The work is satisfactory to the best my knowledge.

Date: 11/05/12

Prof.S.Panigrahi

Department of Physics

National Institute of Technology

Rourkela-769008

ACKNOWLEDGEMENT

I have taken efforts in this project. However, it would not have been possible without the kind support and help of many individuals and organizations. I would like to extend my sincere thanks to all of them. I am highly indebted to **Dr. S.K. Sarangi**, Director, for giving me the opportunity and also my heartfelt thanks and appreciations to The Department of Physics for their guidance and constant supervision as well as for providing necessary equipments regarding the project work & also for their support in completing the project.

No amount of words can adequately express the debt I owe to my Guide, **Dr.S.Panigrahi**, Professor in Physics, NIT Rourkela for his continuous encouragement and thoughtful discussion during the course of present work. I am very grateful to him for giving me the opportunity to work on metal oxide, appreciating my ideas and allowing me the freedom to take on the tasks independently, helping me to explore the things by myself and enriching me with the knowledge amassed.

I would like to express my special gratitude and thanks to **our research scholar Mr.Harinath Aireddy,Mr.Senthil V.Nathan,Mr.Rakesh Muduli & Mrs.Priyambada** for giving me such attention and time. I take this opportunity to express my deep sense of gratitude towards **Mr. Avinna Mishra** for helping me a lot in my characterisation work, who was ever willing to engage in thoughtful discussions and was always ready to help me whenever required. Finally, yet importantly, I would like to express my heartfelt thanks to my beloved parents for their blessings, all the lab members of Physics Department, NIT Rourkela, my friends/classmates for their help and wishes for the successful completion of this project.

Date: 11/05/12

Surya prakash Ghosh

CONTENTS	PAGE NO.
Abstract	1
<u>CHAPTER-1</u>	
1.INTRODUCTION	
1.1Motivation and Backbackground	2-3
1.2Nanotechnology	4
1.2.1.Properties Of Nanomaterials	4
1.2.2.Processing Methods	5-6
1.2.3. Applications	6
1.3. Objective Of Study	7
<u>CHAPTER-2</u>	
2.LITERTURE SURVEY	
2.1. Crystal Structure Of Zno	8-10
2.2.Optoelectronic Property	10-11
2.3.Optical Band Gap	11-12
2.4.Chemically Grown Zno	12-13
2.5.Application Of Zno Nanostructures	14
<u>CHAPTER-3</u>	
3.MATERIAL AND METHODS	
3.1.Experimental	15-17
3.2.Characterisation Techniques	17

3.2.1 Structural Characterisation	18
3.2.2 Optical Characterisation	18
3.2.3 Thermal Analysis.	18
3.3.X-ray DiffractionXRD	19
3.4. Scanning electron microscope (SEM)	20-21
3.5. Transmission electron microscope (TEM)	21-22
3.6. Differential scanning calorimetry (DSC)	22
3.6.1.Working Of DSC	22
3.6.2.Working Of TGA	23
3.7. UV-Visible Spectroscopy	23
3.8.Fouriesr Transform Infrared Spectroscopy (IR).	24

CHAPTER-4

4.RESULT AND DISCUSSION

4.1. X-ray diffraction (XRD)	25-27
4.2.Scanning Electron Microscope(SEM)	28-29
4.3.Transmission Electron Microscopy(TEM)	30
4.4.Fourier Transform Infrared Spectroscopy(FTIR)	31
4.5. UV- Visible spectroscopy)	31-32
4.6. Differential Scanning Colorimetry (DSC) and TGA	32-33

CHAPTER-5

CONCLUSION	34
-------------------	-----------

REFERENCES	35-36
-------------------	--------------

ABSTRACT

In the present work zinc oxide nanoparticles (ZnO) were successfully synthesized by a sol-gel method and zinc acetate dehydrate and triethanolamine (TEA) were used as the precursor materials. Ethanol and ammonium hydroxide takes care for the homogeneity and PH value of the solution and helps to make a stoichiometric solution to get Zinc oxide nanoparticles. The ZnO powder obtained from this method is calcined at 700°C and 900°C temperatures. The samples were characterized by X-ray diffraction (XRD), Scanning Electron Microscopy (SEM), Fourier transform infrared spectroscopy (FTIR), Transmission electron microscopy (TEM), UV- visible spectroscopy and DSC-TG. Results shows that the calcinations temperature significantly affected the crystalline nature, particle size, and optical properties of the processed ZnO nanoparticles. The XRD spectra indicate that the ZnO crystal has a hexagonal wurtzite structure. TEM images agreement with the XRD data shown that the average size of the nanoparticles. The optical properties of the samples are investigated by measuring the UV-VIS absorption at room temperature. With increasing calcinations temperature the band gap of the samples remains almost same, and the size of the particles increases.

Keyword:zinc oxide,sol-gel method,nanopowder,characterization.

Chapter 1

INTRODUCTION

1.1 Motivation and Background

Today, when the world is surmounting on the roof of technology and electronics, mostly dominated by compatible electronic equipments and thereby creating the need for materials possessing versatile properties. After digging the pages of history for the search of such type of material a very common category of material comes out that is “semiconductor”. Since independence of India the family of semiconductors is dominated by our very known elements Germanium(Ge) and Silicon(Si). Germanium get famous due to possession of property like low melting point and lack of natural occurring germanium oxide to prevent the surface from electrical leakage where as silicon dominates the commercial market for its better fabrication technology and application to integrated circuits for different purposes. As time passes on, the rapid growing world demands speed along with technology. This need was very well fulfilled by GaAs which ease the path for the design of high speed and optoelectronic devices. GaAs which is a direct band gap semiconductor possessing higher carrier mobility and higher effective carrier velocity in comparison to Si makes it better suited for optoelectronics devices. But this do not leads to the completion of requirement for the future world, something more is required that is high temperature electronics devices. The world therefore now demands a material that should possess inherent properties like larger band gap, higher electron mobility as well as higher breakdown field strength. So on making investigation about such a material the name of compound comes out is “Zinc Oxide” which is a wide gap semiconductor material very well satisfying the above required properties. Not only has this Zinc oxide possessed many versatile properties for UV electronics, spintronic devices and sensor applications. Also ZnO has been commonly used in its polycrystalline form over hundred years in a wide range of applications. This ignites many research minds all over the world and creates enthusiasm to develop proper growth and processing techniques for the synthesis of Zinc oxide. Zinc oxide is also known as "Lu-Gan-Stone" in China, Zinc oxide has been used in medical treatment for quite number of

years in China. The research on ZnO is catching fire right from the beginning of 1950, with a number of reviews on electrical [1] and optical properties [2] like N-type conductivity, absorption spectra and electroluminescence decay parameter. The nature of excitonic molecule in semiconductors which was discussed by Haynes [3] aiding a key publication by Park et al concerned with excitonic emission of ZnO [4] is the very first footstep put for the growth and development of ZnO research in the mid of 1960. In 1966 the Raman Effect study of ZnO by Damen and Porto [5] leads to the identification of ZnO phonon energies. The decade of 1970 for ZnO passes away in manufacturing of simpler ZnO devices like ceramic varistors, piezoelectric transducers etc. also with a progress in the study of variety of characterization techniques such as cathodluminescence(CL), capacitance – voltage studies(CV), electrical conduction and so on [6-9]. When the researchers got fade off continues work on characterization technique for a decade, search for different growth procedure and techniques begin. In 1980 a lot of work on high quality thin films of ZnO, metallo-organic chemical vapour deposition (MOCVD) [10], spray pyrolysis [11] and radio frequency magnetron sputtering (RF) [12] has been done extensively. Overall much of the research in 1980's attempted to resolve the issues concerning with lack of satisfactory material for device fabrication. But finally at the end of the decade there were no significant increment in the number of papers. The twilight of stars sprinkles and a new era for research of ZnO begins actually in 1990 with a uniform growth in number of publications related to both characterization and growth techniques. In 1990's, newer growth methods were used including pulsed laser deposition (PLD) [13] and molecular beam epitaxy (MBE) [14]. At the end of late 1990 large scale commercial ZnO comes to the picture. In the field of ZnO research the last decade was mainly concerned with optimization of different growth parameters and processing techniques. Thus currently research work related to production of high quality, reproducible P-type conducting ZnO for device application is the main focus. ZnO has now become one of most studied material in the last seven years as it presents very interesting properties for optoelectronics and sensing applications, in nano range synthesis.

1.2 NANOTECHNOLOGY

“The principles of physics, as far as I can see, do not speak against the possibility of manoeuvring things atom by atom.” these are the words which buried the seed for nano-technology in the scientific mind of number of researchers who were attending the talk of famous physicist Richard Feynman in 1959. The word actually signifies our complete control over the matter. Nanotechnology makes us to believe that we would have the ability to create anything that we could precisely define. Eric Drexler, in the early 1980's coined the powerful word nanotechnology. The world of nanotechnology is implanting its footprint in the present decade very rapidly. Between year 1997 and 2005, investment in nanotechnology research and development by governments around the world soared from \$432 million to about \$4.1 billion, and corresponding industry investment exceeded that of governments by 2005 [15-19]. By 2015, products incorporating nanotech will contribute approximately \$1 trillion to the global economy. About two million workers will be employed in nanotech industries, and three times that many will have supporting jobs.

1.2.1 PROPERTIES OF NANOMATERIALS

Nanostructure materials are single phase or multiphase polycrystalline solids with a typical average size of a few nanometers ($1\text{nm} = 10^{-9}\text{m}$). Basically, the range from (1-100)nm is taken as nano-range for convention as per National Nanotechnology Initiative in the US., and the size of hydrogen atom is considered as the lower limit of nano where as upper limit is arbitrary. The grain sizes are so small; a significant volume fraction of the atoms resides in grain boundaries. Material is characterized by a large number of interfaces in which the atomic arrangements are different from those of crystal lattice [15-19]. The basic classification of nonmaterial is done based on the confinement. Bulk structures show no confinement where as nano-wells and nanowires can be obtained by 2-D and 1-D confinement respectively. The quantum realm comes to the picture when there is a 3D confinement and leads to zero dimension quantum structures that is quantum dot.

1.2.2 PROCESSING METHODS

The synthesis of nanomaterial can be well accomplished by two approaches. firstly, by “Bottom Up” method where small building blocks are produced and assembled into larger structures. Where the main controlling parameters are morphology, crystallinity, particle size, and chemical composition. Examples: chemical synthesis, laser trapping, self-assembly, colloidal aggregation, etc and secondly, by “Top Down” method where large objects are modified to give smaller features. For example: film deposition and growth, nano imprint /lithography, etching technology, mechanical polishing etc. the main reason of alteration in different mechanical, thermal and other property is due to increase in surface to volume ratio.

Synthesis of nanomaterial is most commonly done based on three strategies i.e.

- Liquid-phase synthesis.
- Gas-phase synthesis.
- Vapour-phase synthesis.

LIQUID-PHASE SYNTHESIS

Under liquid phase synthesis the techniques used for synthesis are:

- Co-precipitation.
- Sol-gel Processing.
- Micro-emulsions.
- Hydrothermal/Solvo-thermal Synthesis.
- Microwave Synthesis.
- Sono-chemical Synthesis.
- Template Synthesis.

Gas-Phase Synthesis

- Super saturation achieved by vapourizing material into a background gas, then cooling the gas.

Methods using solid precursors

- Inert Gas Condensation
- Pulsed Laser Ablation

- Spark Discharge Generation
- Ion Sputtering

Methods using liquid or vapor precursors

- Chemical Vapour Synthesis
- Spray Pyrolysis
- Laser Pyrolysis/ Photochemical Synthesis
- Thermal Plasma Synthesis
- Flame Synthesis
- Flame Spray Pyrolysis
- Low-Temperature Reactive Synthesis

Nanostructured materials can have significantly different properties, depending on the chosen fabrication route. Each method offers some advantages over other techniques while suffering limitation from the others.

1.2.3.APPLICATIONS

The two concepts necessary for nanotechnology are self-replication and positional control. These could both come from something called a universal assembler. By following the basic principles of nanotechnology a versatile number of devices can be fabricated. A nanotechnological computer can be built which would have the computational power of computers a few years back, and would be smaller than anything we can see with a microscope. In all, this assembler would weigh about $1.66e-15$ grams, which would make it smaller than a common bacterium. Nanotechnology, like every other field, has both a good and bad side. One side of nanotechnology, is that anything that can be precisely defined can be built.[18-22] If someone is hungry, they have but to go to their replication unit, (something that would probably resemble today's microwave in design) and order whatever it is they want. With nanotechnology, there is the possibility of what is called a 'morph' material, a substance made up of tiny little machines that can take on any shape[22]. A table becomes a chair when unexpected company shows up, stairs that turn into ramps for the disabled, but then again, the disabled could have artificial 'nano limbs', that morph into useful tools when necessary. Nanotechnology could help in creating tomorrow's computers. A computer can be designed which have the size of small

organisms and have the computational power of today's personal computers. This would make it possible to fit a full computer into something the shape and size of a piece of paper, including display, voice recognition, and new features that are not available, due to lack of speed and power of today's computers. Clothes that could change colours, toys that changes shape, self-adapting surgical implants, and many other things, that would drastically improve and diversify our abilities and freedom[18-22].

1.3. OBJECTIVE OF STUDY

Scope of this project work was focused on the following steps:

1. Preparation of the ZnO nanoparticles by sol-gel method. Zinc acetate dehydrate and triethanolamine are the precursors materials here.
2. Characterise the crystals structure and pure phase by using XRD diffraction patterns.
3. Investigation of particle size and observing complex crystalline nature of the ZnO by using TEM.
4. Characterise the surface morphology of the ZnO nanoparticles by Scanning Electron Microscopy.
5. Detect the various characteristic functional groups in molecules of synthesized nanomaterial by FTIR spectroscopy analysis.
6. Study the opto-electrical properties by UV-VIS spectroscopy.

CHAPTER 2

LITERATURE SURVEY

2.1. CRYSTAL STRUCTURE OF ZnO

General, Zinc oxide crystallizes in two main forms, hexagonal wurtzite and cubic zinc blende but the (B₄ type) wurtzite structure is obtained only at optimum pressure and temperature[23,28]. In an ideal wurtzite crystal, with a hexagonal close-packed lattice type, has lattice parameters, $a_0 = 0.32495$ nm and $c_0 = 0.52069$ nm, in the ratio of $c_0 / a_0 = 1.602$, and it belongs to the space group of $P63mc$ [23,27] and is characterized by two interconnecting sub lattices of zn^{2+} and o^{2-} where each anion is surrounded by four cations at the corners of a tetrahedron with a typical sp^3 covalent bonding. Among different phases of ZnO, based on the first principle periodic Hartree-Fock linear combination of atomic orbitals theory the wurtzite is found to be the most thermodynamically stable phase[23]. Tetrahedral symmetry plays a vital role for the polarity of ZnO that arises along the hexagonal axis. Piezoelectricity and spontaneous polarization are the direct consequence of polar symmetry of ZnO along the hexagonal axis[23]. The structure of ZnO, can be described as a number of alternating planes composed of tetrahedrally coordinated O^{2-} and Zn^{2+} ions, stacked alternately along the C-axis (Figure.2.1.)The oppositely charged ions produce positively charged(0001)-Zn and negatively charged $(000\bar{1})$ -O polar surfaces, resulting in a normal dipole moment and spontaneous polarization along the c-axis, as well as a divergence in surface energy [25-26].The polar faces are more stable than non polar faces. The root cause for the natural N-type nature of ZnO is due to the sensitiveness of ZnO lattice constants to the presence of structural point defects (vacancies and interstitials) and extended defects (threading/planar dislocations) that are commonly found in ZnO resulting in a non-stoichiometric compound $Zn_{1+d}O$ with an excess zinc .These excess zinc atoms have the tendency to function as donor interstitials that give its natural N-type conductivity. In ionic form, the excess zinc exist as Zn^+ interstitials that are mobile and they tend to occupy special interstitial sites with Miller index $(\frac{1}{3}, \frac{2}{3}, 0.875)$ as shown in Figure.2.2.These

special sites offer passage routes for zinc interstitials to easily migrate within the ZnO wurtzite structure[36].

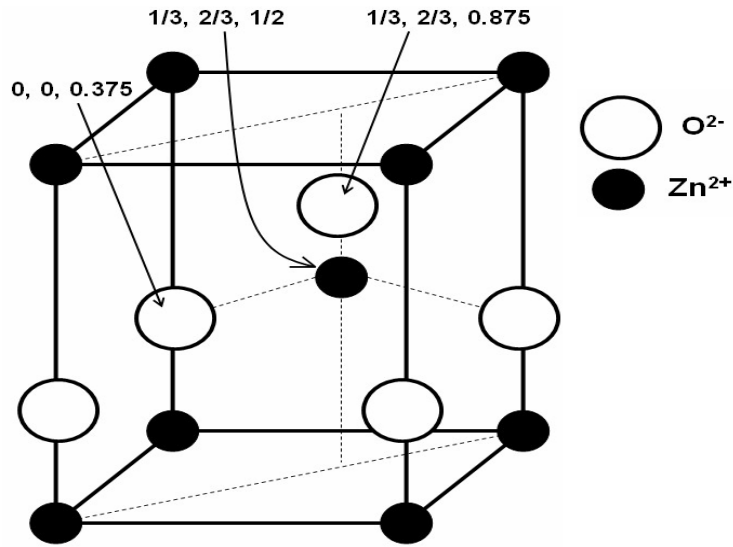


Figure 2.1. ZnO unit cell with ionic positions of zinc and oxygen atoms. Redrawn from [47]

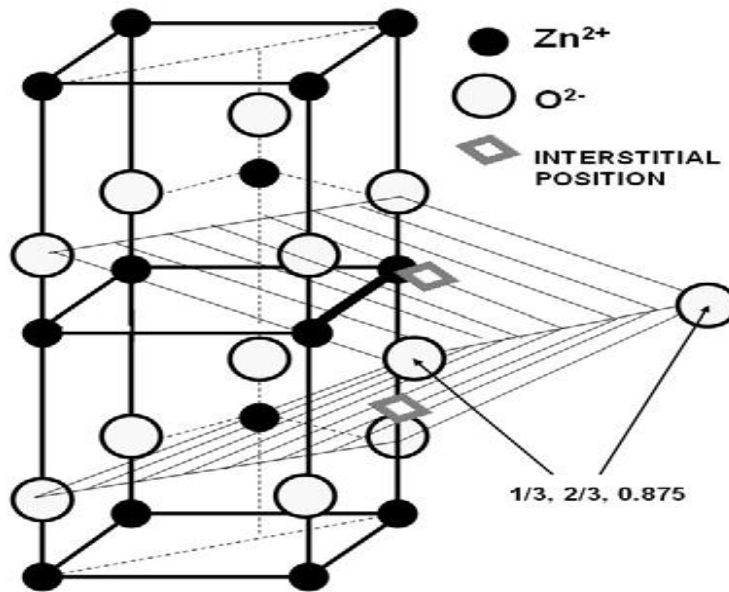


Figure 2.2. Zinc interstitial sites in the ZnO wurtzite lattice. Redrawn from [47]

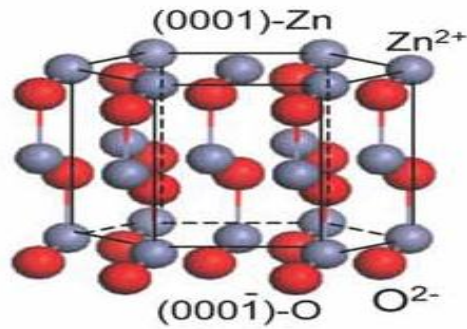


Figure.2.3.The wurtzite structure model of ZnO. The tetrahedral coordination of Zn-O is shown. [28]

2.2 OPTOELECTRONIC PROPERTY

The most important factor responsible for a material to show a better optoelectronic property is the large exciton binding energy and this property is possessed by Zinc oxide having binding energy of 60mev which could be attended at and above room temperature due to excitonic recombination[29]. The process of optical absorption and emission have been influenced by bound excitons which are extrinsic transition related to dopants or defects thereby usually responsible for creating discrete electronic states in the band gap. Theoretically, neutral or charged donors and acceptors are the members by which exciton could be bound with and it merely depends on the band structure of semiconductor material[29,30]. Thus exciton which is a bound system it do not requires traps to localize carriers and recombines with high efficiency. The piezoelectrically induce field makes deeper exciton of ZnO more stable against field ionization. Magnesium doped zinc oxide possesses a wide range of sensing spectra between (200-280)nm which makes it suitable to tune for UV-B and UV-C and can be made applicable for various fields such as solar UV radiation monitoring, ultrahightemperature flame detection etc[24]. Zinc oxide films made from single crystal shows directionally dependent optical properties due to which it can be applied for modulation of UV radiation. The current example of it is the designed model of ZnO modulator with a contrast of 70:1 and operation speed of 100ps [24]. Also high breakdown stress and high saturation velocity of zinc oxide increases its demand for the different electronic application. PL spectra of ZnO nanowire shows increase of green emission intensity with a decrease of nanowire diameter and continuous

reduction of diameter of ZnO nanowire gives quantum size effect and due to this size confinement exciton binding energy is enhanced. Transport characteristics and interaction of phonon with free carrier have impact on the performance of optoelectronic devices which can be acquired by the knowledge of vibrational properties of the material. The excellent emitting power of ZnO has been investigated through different reports and line width of excitonic recombination is as narrow as 40 μeV with fine spectroscopic details have been observed. The refractive index of wurtzite ZnO as reported [23,27] is $n_w = 2.008$ and $n_e = 2.029$ [36].

2.3.OPTICAL BAND GAP

As reported from various literatures the band gap of ZnO films mostly depends on the carrier concentration and is found to be 3.37eV on basis of carrier concentration of 10^{18} – $10^{20}/\text{cm}^3$. Anomalous change(increase) in band gap has been observed when the carrier concentration is $5 \times 10^{18}/\text{cm}^3$, and then a sudden decline in band gap [23,24],when concentration changes to 3 – $4 \times 10^{19}/\text{cm}^3$.Quantum confinement of electrons in small grains created by potential barriers at the grain boundaries are thought to responsible for the drastic change in band gap. Sometimes also at higher doping concentration on a blue shift towards shorter wavelength has been observed and can be explained on the basis of Burstein–Moss effect[30,31].According to which increase of the carrier concentration due to Al doping results in a shift of the Fermi level and block some of the lowest states, thereby causing widening of the band gap resulting in the blue-shift of the absorption tail. The band gap of ZnO as calculated by local density approximation (LDA) is found to be 3.77eV which mostly accounts for the Zn 3d electrons [23,24] as shown in the figure.2.4. The ZnO having direct band gap is very well indicated by the valence band maxima and lowest conduction band minima both occurring at the same Γ point of $k=0$.Zn 3d levels are indicated by bottom ten bands (occurring around 9eV) and O 2p bonding states are highlighted by next six bands from -5eV to 0 eV. The empty Zn 3s levels signified by first two conduction band states are mainly Zn localized. Crystallization of ZnO mostly favourable in wurtzite symmetry and crystal field splitting as well as spin orbit interaction results in three states say A, B & C figure.2.4.The symmetry of the A valence sub band is considered to be Γ_7 based on the polarization properties of the free exciton transitions where as contradicting to it the most recent magneto-optical studies of the free exciton transition fine structure interpreted the symmetry to be Γ_9 . But the controversy is continuing as before 40 years ago. It has been

reported in undoped films grown by MBE a new line at 3.32 eV was reported (ZnO on CaF₂ (111)) which is quite close to the 3.35 eV line for ZnO on *a*-plane sapphire presented by Kato et al. [11] (taking into account the different strain situations in the films). Both groups [10-11] assigned the recombination as caused by excitons bound to neutral acceptors.

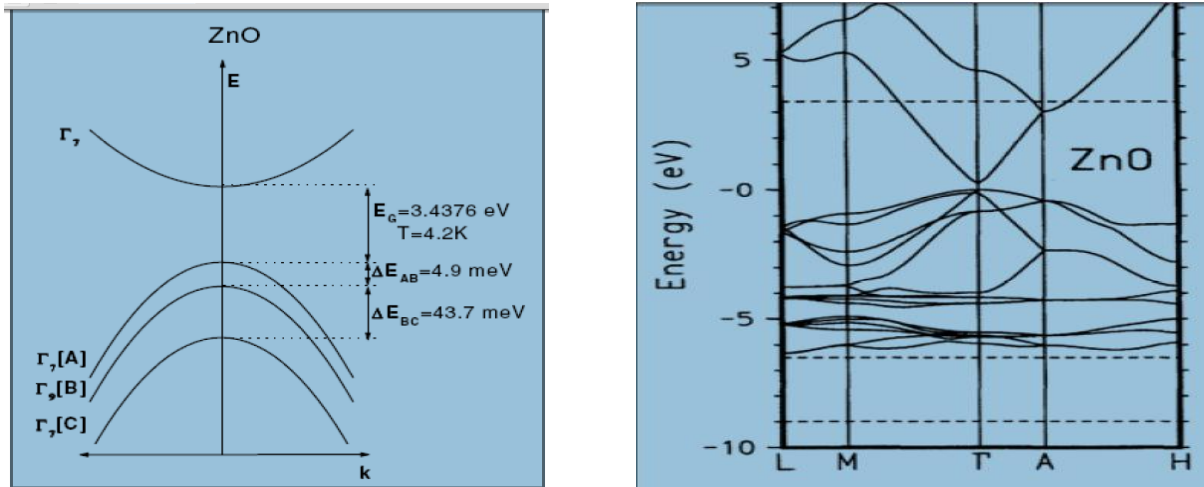


Figure.2.4. (a) Band structure and symmetries of hexagonal ZnO. The splitting into three valence bands (A, B, C) is caused by crystal field and spin-orbit splitting.[29]. (b) The LDA band structure of bulk wurtzite ZnO calculated using standard pseudopotentials [23]

2.4. CHEMICALLY GROWN ZnO

As we all know any material in its nano form is more demandable than in its bulk form because in nano level the material undergoes a drastic change in its property and has versatile application. Thus zinc oxide which is a multifunctional material with a large direct band gap created anxiousness in the scientific minds to enhance the research on one dimensional nanostructure especially oxide materials. The properties of zinc oxide makes the material eligible exists in various shapes in the form of nanostructures exhibiting a varieties of properties like piezoelectricity, optical transparency, conductivity, solar cell, UV and visible photoluminescence, optical nonlinearity and many more. But obtaining various shapes of nanostructures merely depends on different processing techniques. Methods which are related to the synthesis of various shapes of zinc oxide nanostructures are chemical and thermal vapour deposition laser ablation, vacuum arc deposition, electrochemical, and hydrothermal process. But all these

methods reported possesses many complex steps; require sophisticated equipments and rigorous experimental conditions[33]. Thus need for a synthesis technique arises which would be simple and by using it zinc oxide nanostructures can be grown in a laboratory environment and also characterized such structures for a wide range of applications through repeated fabrication and modification. One such inexpensive method which can be implemented without having any complexes and need for sophisticated equipments is also not desirable is the wet chemical method. Not only the method enable us to fabricate multi-dimensional nanostructures in a large scale but also provides repeated preparation that enables one to varying the process conditions for an investigational study and repeatability in the yield. Till now there were number of reports regarding the fabrication of one dimensional ZnO nanostructures especially nanorods and nanotubes via number of routes. Some of them are Mohanta et al. have reported the fabrication of ZnO nanorods grown on P-type GaN/sapphire and silicon-on-insulator substrates by chemical vapour deposition [32]. The nanorods show strong UV band edge emission around 380nm [35-37]. In another report by Ding et al., ZnOnanorods have been grown on various substrates (ceramic, glass, Si, metal) by solution phase growth at 95°C[36]. However there are only few reports on the fabrication of ZnO nanobelts by VLS and thermal evaporation method [37-40]. Zhang et al. have fabricated ZnO nanobelts by thermal evaporation of ZnCl₂ at 700 °C under flow of Ar and O₂ [39]. VLS method is also adapted to fabricated ZnOnanobelts, but only very few literature are there which talks about the fabrication of ZnOnanobelts by chemical/hydrothermal method.

But as this chemical method is concerned it is found to be very simple, cost-effective and quite suitable to adopt in the laboratory without much infrastructures. By adapting this method it has been possible to grow ZnO nanobelts at room temperature over a very short duration of growth of 4 hrs only and without using any surfactant or catalyst Not only this much but this method does not necessitate the maintenance of rigorous experimental conditions as in the earlier cases[40-42]. Therefore, overall we can conclude that synthesis of ZnO nanostructures by chemical route not only provides a method for large-scale fabrication of ZnOnanorods with a low cost, but also open a way to the size-controlled fabrication of other materials.

2.5.APPLICATION OF ZnO NANOSTRUCTURES

Zinc oxide due to its versatility and multifunctionality creates attention in the research field related to its applications. A wide number of synthesis techniques also been developed by which ZnO can be grown in different nanoscale forms and thereby different novel nanostructures can be fabricated with different shapes ranging from nanowires to nanobelts and even nanosprings. Generally, nanobelts of ZnO can be obtained by sublimation of ZnO nanopowder without any catalyst. Each property of ZnO has its own applications. Starting from the wide band gap of ZnO makes it enable to form clusters consisting of ZnO nanocrystals and ZnO nanowires. Also due to the wide band gap, synthesis of P–N homojunctions has been reported in some literatures but clarity on stability and reproducibility has not been established yet. Many fine optical devices can be fabricated based on the free-exciton binding energy in ZnO that is 60 meV because large exciton binding energy makes ZnO eligible to persist at room temperature and higher too. Since ZnO crystals and thin films exhibit second- and third-order non-linear optical behaviour, it can be used for non-linear optical devices. Third-order non-linear response has recently been observed in ZnO nano-crystalline films which make it suitable for integrated non-linear optical devices. Generally, the advantage of tuning the physical property of these oxides like zinc oxide becomes the root cause for the synthesis of smart application device. the electrical, optical, magnetic, and chemical properties can be very well tuned by making permutation and combination of the two basic structural characteristics they possess the is cations with mixed valence states, and anions with deficiencies (vacancies). Thus, making them suitable for several application fields such as semiconductor, superconductor, ferroelectrics, and magnetic. DSSCs is an optoelectronics device that converts light to electrical energy *via* charge separation in sensitizer dyes absorbed on a wide band gap semiconductor, which is different to conventional cells[23]. One important difference between conventional and dry sensitized solar cell is that they are epitomized by silicon p-n junction solar cells. The demand for zinc oxide based dye-sensitized solar cell is due to its low fabrication cost.

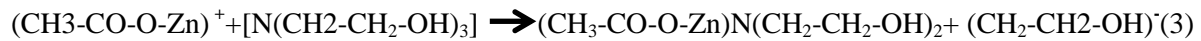
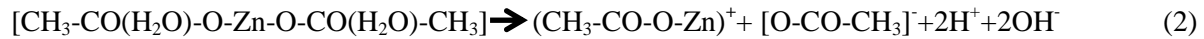
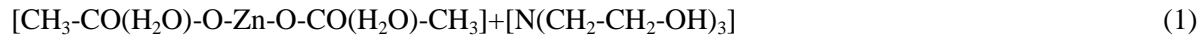
CHAPTER -3

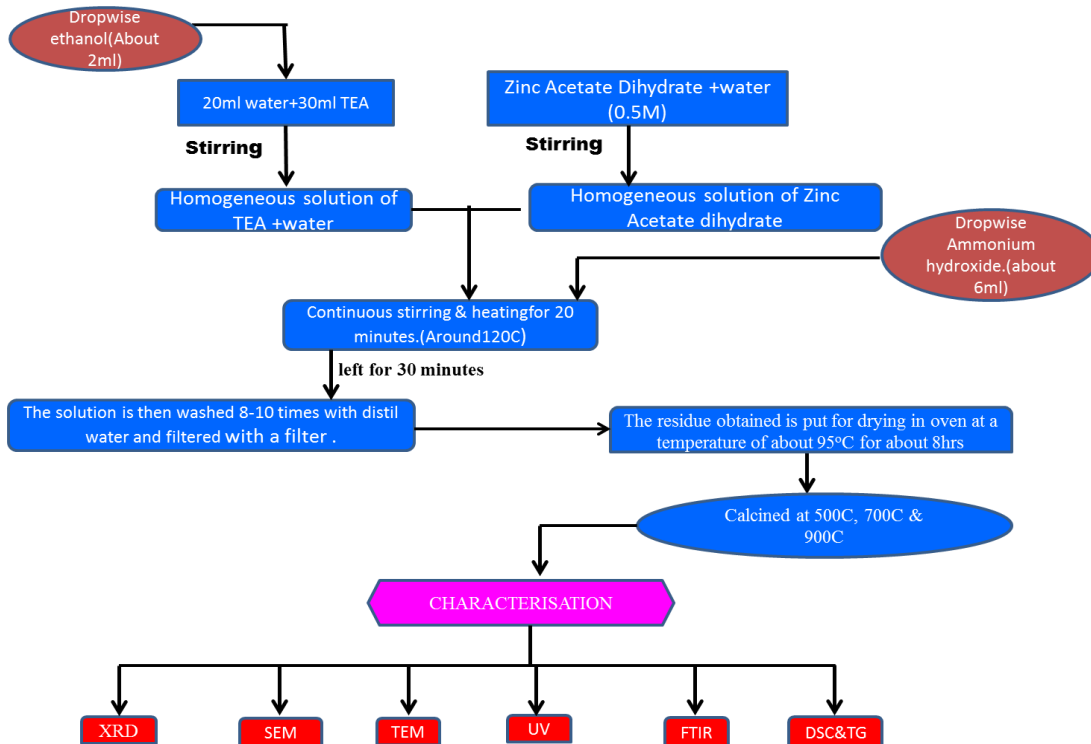
MATERIALS AND METHODS

3.1 EXPERIMENTAL

The precursors used in the synthesis ZnO by sol-gel process are Zinc acetate dehydrate having purity 99%. The need for surfactant is fulfilled by the use of triethanolamine (TEA) which also possesses 99% purity. Ethanol and ammonium hydroxide takes care for the homogeneity and PH value of the solution and helps to make a stoichiometric solution to get Zinc oxide nanoparticles[17]. All the chemicals were supplied by Rankem chemicals Ltd. Firstly, in a 100ml beaker 20 ml of water is added with 30ml of TEA and dropwise ethanol is added with continuous stirring to get a homogeneous solution. After addition of 100 drops ethanol that is about 2ml and continuous stirring results a homogeneous solution. Keeping the stoichiometry in mind a 2gm batch of zinc oxide is prepared. Firstly, 30ml of water is mixed with 20 ml of TEA with constant stirring and dropwise addition of ethanol. The homogeneous solution obtained is kept for 2-3 hrs. Simultaneously, as per the molar calculation for 2gm batch of zinc oxide 5.39gm of zinc acetate di-hydrate is mixed with 50ml water and 0.5M of solution is prepared which is subjected to continuous stirring to get a homogeneous solution. Now the two solutions are mixed together in 500ml beaker and drop wise ammonium hydroxide is added with continuous heating and stirring for 20minutes. About 10ml of distil water is added during stirring. Then the solution is left for 30 minutes which results in the formation of white bulky solution. The solution is then washed 8-10 times with distil water and filtered in a filter paper. The residue obtained is put for drying in oven at a temperature of about 95°C for 8hrs. The yellowish white powder obtained is subjected to calcinations at three different temperatures 500°C, 700°C and 900 °C for 4hrs.

The growth of ZnO from zinc acetate dihydrate precursor using sol-gel process generally undergoes four stages, such as solvation, hydrolysis, polymerization and transformation into ZnO. The zinc acetate dihydrate precursor was first solvated in ethanol, and then hydrolyzed, regarded as removal of the intercalated acetate ions and results in a colloidal-gel of zinc hydroxide (Eq. (5)), size and activity of solvent have obvious influence on the reacting progress and product. Ethanol has smaller size and a more active –OH. Ethanol can react more easily to form a polymer precursor with a higher polymerization degree, which is required to convert sol into gel [49]. These zinc hydroxide splits into Zn²⁺ cation and OH⁻ anion according to reactions (Eq. (4)) and followed by polymerization of hydroxyl complex to form “Zn–O–Zn” bridges and finally transformed into ZnO (Eq. (5)) [48]





The calcinated powders are studied using different characterisation techniques. Confirmation of pure ZnO phase is verified by XRD analysis. The shape and morphology of particles are studied by SEM pictures obtained. Whether the particles have attended the nano range is studied by taking the TEM pictures of sample which gives the sharp peaks in XRD analysis. The report of DSC & TG gives the information about the thermal decomposition of sample. Finally, absorption spectroscopy and Fourier transform infrared (FTIR) spectroscopy were performed and the results are studied to understand the optoelectronic property of sample prepared.

3.2 .CHARACTERISATION TECHNIQUES

In order to investigate various properties of the prepared sample, it has to goes under a number of characterisation techniques. The results of which gives the information about the different optical and structural properties of sample.

3.2.1 STRUCTURAL CHARACTERISATION

In order to get exact information about the crystal structure, surface morphology, particle size etc. the following characterisation techniques are applicable.

- XRD (X-ray Diffraction)
- SEM (Scanning electron microscope)
- Transmission electron microscope (TEM)

3.2.2.OPTICAL CHARACTERISATION

As we know zinc oxide has wide range of application in the field of optoelectronics devices on putting the sample to following characterisation techniques gives information related to optical properties.

- UV-Visible Spectroscopy
- Fourier Transform Infrared Spectroscopy (IR).

3.2.3 THERMAL ANALYSIS

- DSC&TG

3.3.XRD (X-ray Diffraction)

Upto 1895 the study of matter at the atomic level was a difficult task but the discovery of electromagnetic radiation with 1 \AA (10^{-10} m) wavelength, appearing at the region between gamma-rays and ultraviolet, makes it possible. As the atomic distance in matter is comparable with the wavelength of X-ray, the phenomenon of diffraction find its way through it and gives many promising results related to the crystalline structure. The unit cell and lattices which are distributed in a regular three-dimensional way in space forms the base for diffraction pattern to occur. These lattices form a series of parallel planes with its own specific d-spacing and with different orientations exist. The reflection of incident monochromatic X-ray from

successive planes of crystal lattices when the difference between the planes is of complete number n of wavelengths leads to famous Bragg's law:

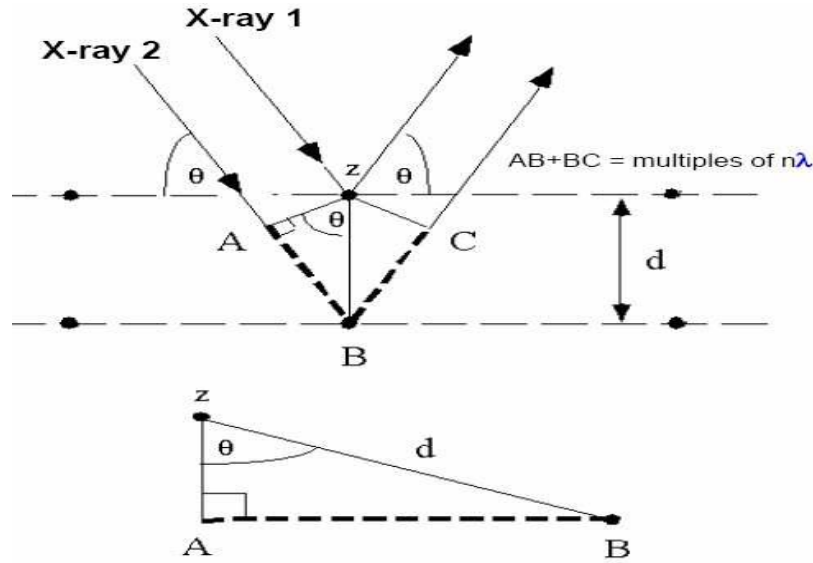


Figure3.1.X-ray Diffraction in accordance with Bragg's Law

$$n \lambda = 2d \sin \theta$$

Where n is an integer 1, 2, 3..... (Usually equal 1), λ is wavelength in angstroms (1.54 Å for copper), d is interatomic spacing in angstroms, and θ is the diffraction angle in degrees. Plotting the angular positions and intensities of the resultant diffracted peaks of radiation produces a pattern, which is characteristic of the sample. The fingerprint characterization of crystalline materials and the determination of their structure are the two fields where XRD has been mostly used. Unique characteristic X-ray diffraction pattern of each crystalline solid gives the designation of “fingerprint technique” to XRD for its identification. XRD may be used to determine its structure, i.e. how the atoms pack together in the crystalline state and what the interatomic distance and angle are etc. From these points it can be concluded that X-ray diffraction has become a very important and powerful tool for the structural characterization in solid state physics and materials science.

3.4. SEM (Scanning electron microscope)

The scanning electron microscope (SEM) uses a focused beam of high-energy electrons to generate a variety of signals at the surface of solid specimens. The signals that derive from electron reveal information about the sample including external morphology (texture), chemical composition, and crystalline structure and orientation of materials making up the sample. In most applications, data are collected over a selected area of the surface of the sample, and a 2-dimensional image is generated that displays spatial variations in these properties. Areas ranging from approximately 1 cm to 5 microns in width can be imaged in a scanning mode using conventional SEM techniques (magnification ranging from 20X to approximately 30,000X, spatial resolution of 50 to 100 nm). The SEM is also capable of performing analyses of selected point locations on the sample; this approach is especially useful in qualitatively or semi-quantitatively determining chemical compositions (using EDS), crystalline structure, and crystal orientations (using EBSD)[50,53]. The design and function of the SEM is very similar to the EPMA and considerable overlap in capabilities exists between the two instruments.[53]

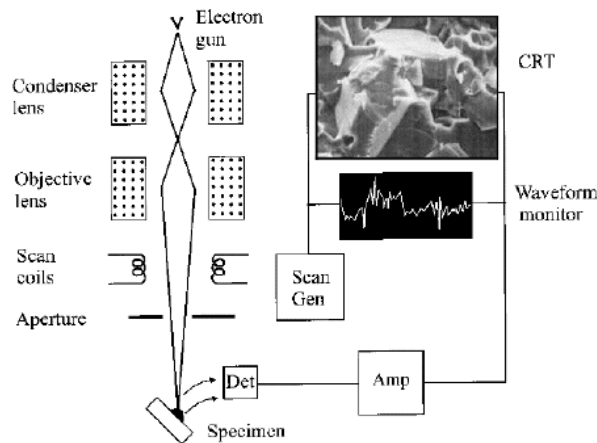


Figure3.2. Schematic Diagram of SEM.

Accelerated electrons in an SEM carry significant amounts of kinetic energy, and this energy is dissipated as a variety of signals produced by electron-sample

interactions when the incident electrons are decelerated in the solid sample. These signals include secondary electrons (that produce SEM images), backscattered electrons (BSE), diffracted backscattered electrons (EBSD that are used to determine crystal structures and orientations of minerals), photons (characteristic X-rays that are used for elemental analysis and continuum X-rays), visible light (cathodoluminescence--CL), and heat. Secondary electrons and backscattered electrons are commonly used for imaging samples: secondary electrons are most valuable for showing morphology and topography on samples and backscattered electrons are most valuable for illustrating contrasts in composition in multiphase samples (i.e. for rapid phase discrimination). SEM analysis is considered to be "non-destructive"; that is, x-rays generated by electron interactions do not lead to volume loss of the sample, so it is possible to analyze the same materials repeatedly. The SEM is routinely used to generate high-resolution images of shapes of objects (SEI) and to show spatial variations in chemical compositions: 1) acquiring elemental maps or spot chemical analyses using EDS, 2) discrimination of phases based on mean atomic number (commonly related to relative density) using BSE, and 3) compositional maps based on differences in trace element "activators" (typically transition metal and Rare Earth elements) using CL[86]. The SEM is also widely used to identify phases based on qualitative chemical analysis and/or crystalline structure. Precise measurement of very small features and objects down to 50 nm in size is also accomplished using the SEM.

3.5. Transmission electron microscope (TEM)

Electron Microscopes are scientific instruments that use a beam of highly energetic electrons to examine objects on a very fine scale. This examination can yield the information like topography, morphology, composition as well as crystallographic information's. Working principle is exactly as their optical counterparts except that they use a focused beam of electrons instead of light to "image" the specimen and gain information as to its structure and composition. The main use of this technique is to examine the specimen structure, composition or properties in submicroscopic details so that this microscopy technique is significantly involved in numerous fields. In TEM there is no change in the refractive index of the medium when the illumination beam is deflected, the vacuum in the lens is the same as the vacuum in the column. Deflection is in this case only due to the electromagnetic properties of the lens which are defined by electromagnetic plates that are only able to influence the path direction of the electrons, since all

of the electrons carry a negative charge[54]. Those electrons that pass through the sample go on to form the image while those that are stopped or deflected by dense atoms in the specimen are subtracted from the image. In this way a black and white image is formed. Remaining other electrons which pass close to heavy atom and get only slightly deflected make their way down the column and contribute to the image.. There are three main reasons why the microscope column must be operated under very high vacuum. The first of these is to avoid collisions between electrons of the beam and stray molecules. Such collisions can result in a spreading or diffusing of the beam or more seriously can result in volatilization event if the molecule is organic in nature. Such volatilizations can severely contaminate the microscope column especially in finely machined regions such as apertures and pole pieces that will serve to degrade the image.

3.6. Differential scanning calorimetry (DSC)

Thermal Analysis (TA) generally refers to the simultaneous application of Thermogravimetry (TGA) and Differential scanning calorimetry (DSC) to one and the same sample in a single instrument. The test conditions are perfectly identical for the TGA and DSC signals (same atmosphere, gas flow rate, vapour pressure of the sample, heating rate, thermal contact to the sample crucible and sensor, radiation effect, etc.)[57]. Thus, Thermal analysis (TA) is a group of techniques in which changes of physical or chemical properties of the sample are monitored against time or temperature, while the temperature of the sample is programmed which may involve heating or cooling at a fixed rate, holding the temperature constant (isothermal), or any sequence of these.

3.6.1. WORKING OF DSC

The sample and reference chambers are heated equally into a temperature regime in which a transformation takes place within the sample. As the sample temperature deviates from the reference temperature, the device detects it and reduces the heat input to one cell while adding heat to the other, so as to maintain a zero temperature difference between the sample and reference. The quantity of electrical energy per unit time which must be supplied to the heating element in order to maintain null balance is assumed to be proportional to the heat released per unit time by the sample.

3.6.2. WORKING OF TGA

Measurements of changes in sample mass with temperature are made using a thermobalance. This is a combination of a suitable electronic microbalance with a furnace and associated temperature programmer. The balance should be in an enclosed system so that the atmosphere can be controlled. Y axis is %mass loss; X axis is temp (or time, since usually a linear heating rate).

As the specimen changes weight, its tendency to rise or fall is detected by LVDT. A current through the coil on the counterbalance side exerts a force on the magnetic core which acts to return the balance pan to a null position. The current required to maintain this position is considered proportional to the mass change of the specimen

3.7. UV-VISIBLE SPECTROSCOPY

The wavelength of UV is shorter than the visible light. It ranges from 100 to 400 nm. In a standard UV-V is spectrophotometer, a beam of light is split; one half of the beam (the sample beam) is directed through a transparent cell containing a solution of the compound being analysed, and one half (the reference beam) is directed through an identical cell that does not contain the compound but contains the solvent. The instrument is designed so that it can make a comparison of the intensities of the two beams as it scans over the desired region of the wavelengths. If the compound absorbs light at a particular wavelength, the intensity of the sample beam (I_s) will be less than that of the reference beam[51]. Absorption of radiation by a sample is measured at various wavelengths and plotted by a recorder to give the spectrum which is a plot of the wavelength of the entire region versus the absorption (A) of light at each wavelength. And the band gap of the sample can be obtained by plotting the graph between ($\alpha h\nu$ vs $h\nu$) and extrapolating it along x-axis. Ultraviolet and visible spectrometry is almost entirely used for quantitative analysis; that is, the estimation of the amount of a compound known to be present in the sample. The sample is usually examined in solution.

3.8.FOURIER TRANSFORM INFRARED SPECTROSCOPY (FTIR).

In the region of longer wavelength or low frequency the identification of different types of chemicals is possible by this technique of infrared spectroscopy and the instrument requires for its execution is Fourier transform infrared (FTIR) spectrometer. The spectroscopy merely based on the fact that molecules absorb specific frequencies that are characteristic of their structure termed as resonant frequencies, i.e. the frequency of the absorbed radiation matches the frequency of the bond or group that vibrates. And the detection of energy is done on the basis of shape of the molecular potential energy surfaces, the masses of the atoms, and the associated vibronic coupling. Sometimes help of approximation techniques like Born–Oppenheimer and harmonic approximations are also taken. As each different material is a unique combination of atoms, no two compounds produce the exact same infrared spectrum. Therefore, infrared spectroscopy can result in a positive identification (qualitative analysis) of every different kind of material. In addition, the size of the peaks in the spectrum is a direct indication of the amount of material present[55-56]. FTIR can be used to analyze a wide range of materials in bulk or thin films, liquids, solids, pastes, powders, fibers, and other forms. FTIR analysis can give not only qualitative (identification) analysis of materials, but with relevant standards, can be used for quantitative (amount) analysis. FTIR can be used to analyze samples up to ~11 millimeters in diameter, and either measure in bulk or the top ~1 micrometer layer. FTIR spectra of pure compounds are generally so unique that they are like a molecular "fingerprint".

CHAPTER-4

RESULT AND DISCUSSION

4.1. X-ray diffraction (XRD)

Figure.4.1 (a),(b) & (c) gives the X-ray diffraction pattern for samples S1,S2 & S3 calcined at 500°C, 700°C and 900°C respectively. Study of standard data JCPDS 76-0704 confirmed that the synthesized materials are hexagonal ZnO phase (wurtzite Structure).The pattern was indexed with hexagonal unit cell structure with P63mc and the lattice parameters are given as follows:

	500°C	700°C	900°C
a	3.2488 Å	3.2530 Å	3.2499Å
b	3.2488 Å	3.2530 Å	3.2499 Å
c	5.2054 Å	5.2130 Å	5.2066 Å
c/a	1.6022 Å	1.6025 Å	1.6020 Å

Table.4.1(a) shows the variation of lattice parameters with Calcination Temperature

The deviation of the lattice parameters is caused may be due to presence of various point defects such as zinc antisites, oxygen vacancies, and extended defects, such as threading dislocation. With increasing calcination temperature from 500°C to 900°C peak height increases and FWHM decreases as result diffraction peaks become stronger and sharper, thereby indicating that the crystal quality has been improved and the size of particles become bigger. The table below shows the variation of peak height and FWHM with different annealing temperature. The result has been shown for only high intensity peak.

	CalcinationTemp(°C)	Peak height	FWHM(°)
S1	500	105.61	0.2755
S2	700	163.73	0.2362
S3	900	166.01	0.1968

Table.4.1(b) shows the variation of peak height and FWHM with calcination Temperature

Diffraction lines of ZnO were broadened, and diffraction broadening was found dependent on Miller indices of the corresponding sets of crystal planes. For most samples the diffraction line (0 0 2) is narrower than the line (1 0 1), and (1 0 1) is narrower than the line (1 0 0). This indicated an asymmetry in the crystallite shape. The average crystallite sizes of samples S2(700°C) and S3(900°C) were determined by the Debye-Scherrer formula $0.9\lambda/B\cos(\theta)$ and were found to be 26.74 nm and 28.93 nm respectively. With increasing temperature crystallinity of the particles increases causing particles become bigger. Thus, in order to get smaller particles lower temperature is favourable. And comparing the xrd report of three samples it has been concluded that samples calcined at 700°C and 900°C gives high intensity fine peaks, which can be used for further characterization.

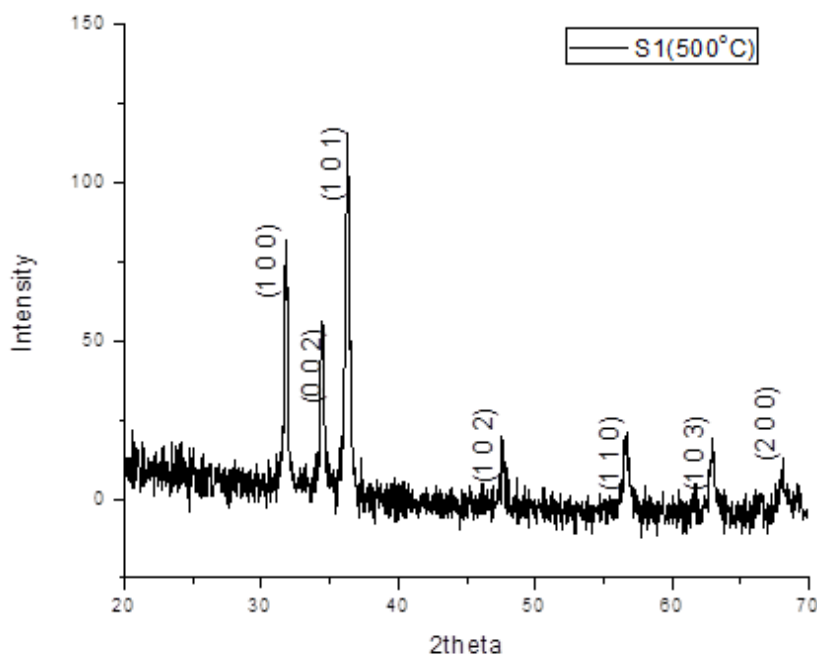


Figure 4.1(a) XRD pattern of ZnO nanoparticles synthesized at calcinizing temperatures 500°C.

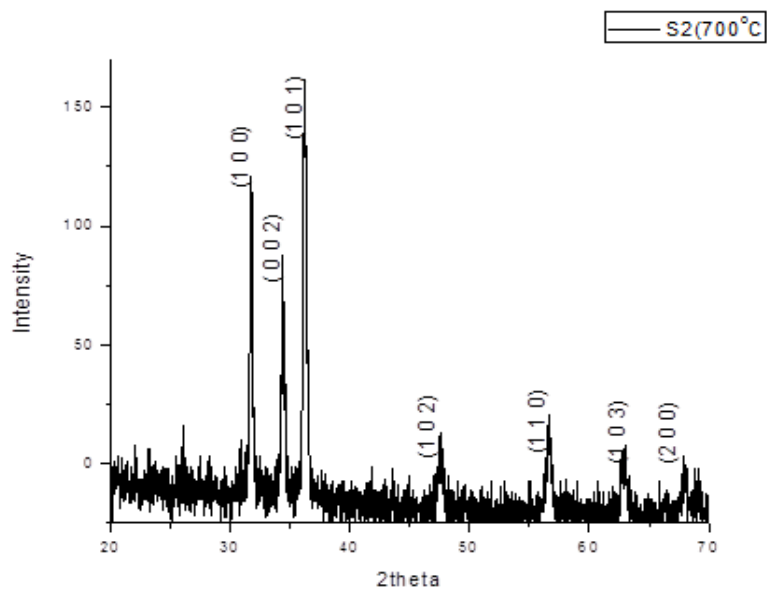


Figure 4.1(b) XRD pattern of ZnO nanoparticles synthesized at calcinizing temperatures 700°C

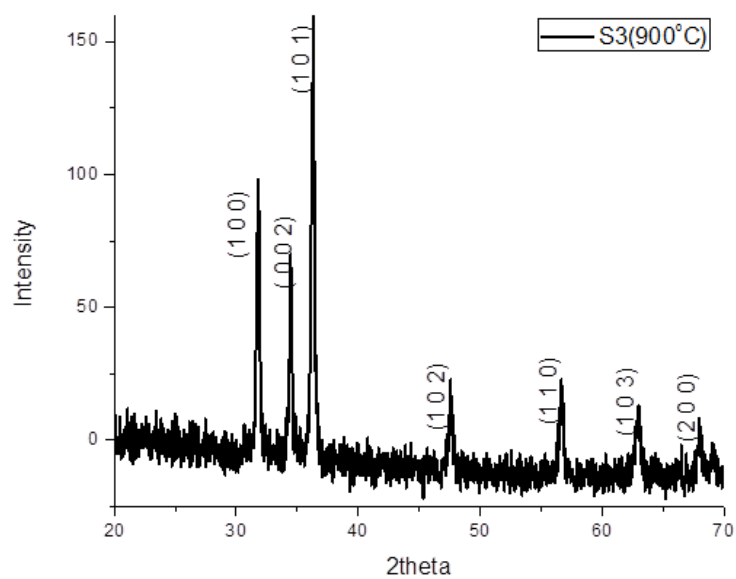


Figure 4.1(c) XRD pattern of ZnO nanoparticles synthesized at calcinizing temperatures 900°C

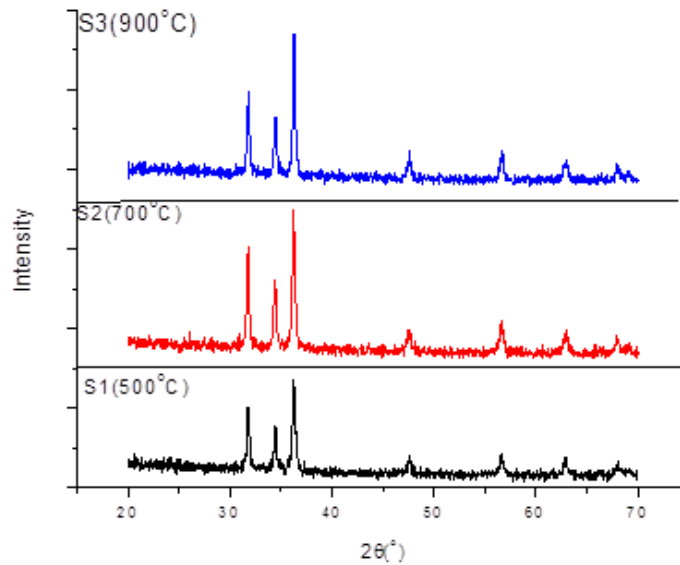


Figure.4.1(d) Comparison of XRD for three sample S1,S2 &S3 calcined at 500°C ,700°C & 900°C respectively.

4.2.Scanning Electron Microscope(SEM)

Figure.4.2(a) & (b) shows the SEM morphology of the synthesized nano ZnO particles at different calcining temperatures. It demonstrates clearly the formation of spherical ZnO nanoparticles, and change of the morphology of the nanoparticles with the calcination temperature. The secondary ZnO(average size $\sim 1 \mu\text{m}$) particles as observed by SEM images consist of primary ZnO nanocrystallites ($\sim 20 \text{ nm}$) was estimated by line intersecting method. The primary nanocrystallites are combined to form a larger particle (secondary) by the following two routes [16]: (1) Fusion of one primary crystallite ($\sim 20 \text{ nm}$) into another. (2) Aggregation of the primary crystallites ($\sim 20 \text{ nm}$).

The first mechanism gives large crystallite size of micrometer scale ($\sim \mu\text{m}$). The second route results a bigger particle consisting of primary ($\sim 20 \text{ nm}$) subunits with less porosity. Nucleation and growth rate increases with increase in annealing temperature, as a result agglomeration is more in the sample annealed at 900°C. In the present work it appears that the aggregation is the

dominant mechanism which occurred during the crystallization of gel-network leading to macroscopic ZnO particles.

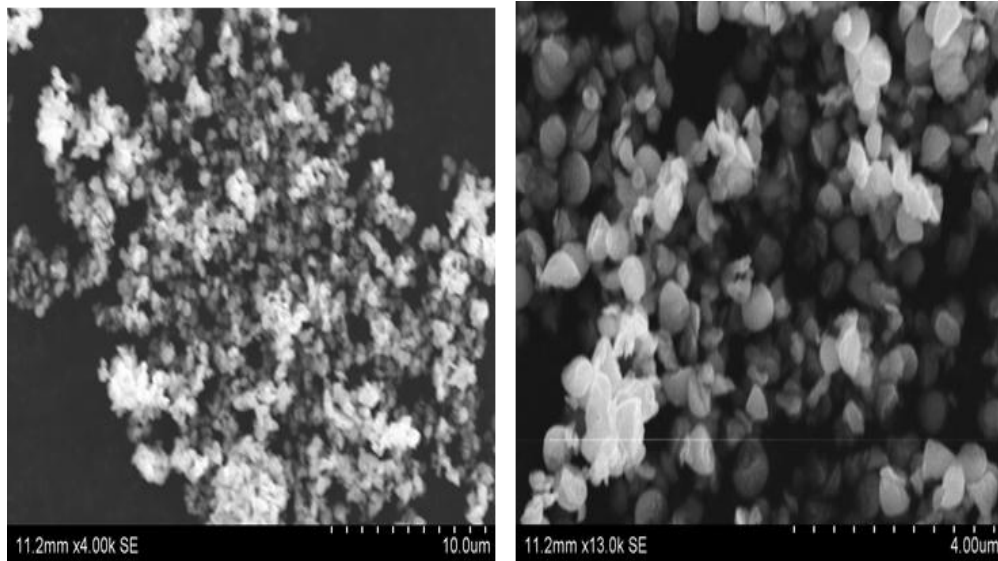


Figure.4.2(a) SEM of sample calcined at 700°C for 4hrs.

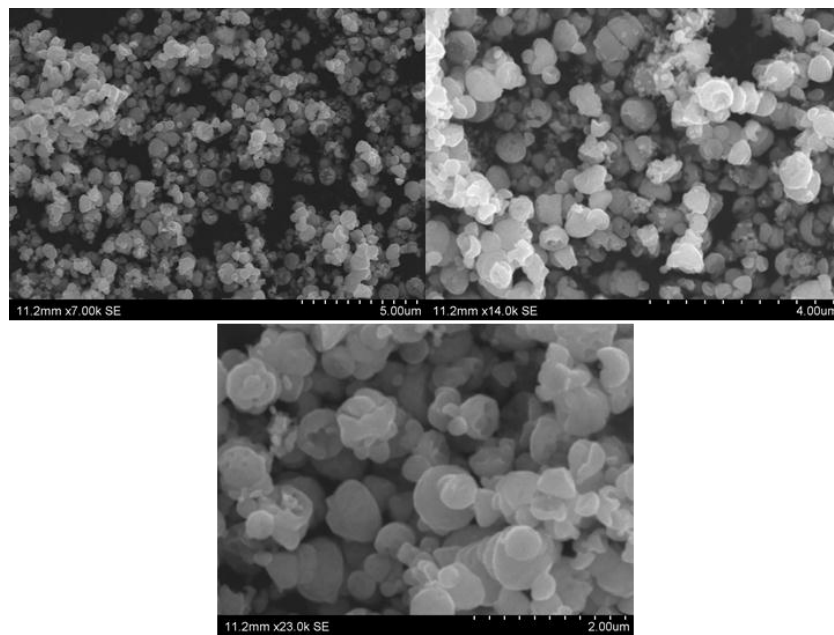


Figure4.2(b)The SEM images clearly show microstructural homogeneities and remarkably different morphology for ZnO powder calcined at 900°C for 4h.

4.3. Transmission Electron Microscopy(TEM)

Figure 4.3(a), & 4.3(b) shows the TEM images and selected area electron diffraction patterns of ZnO nanoparticles annealed at 700°C and 900°C. This image reveals that the product consist of spherical particles with the average size of 35-45 nm which is in close agreement with that estimated by Scherer formula based on the XRD pattern. From the Figure 4.3(a), & 4.3(b) the selected area electron diffraction(SAED) shows the crystalline structure complexity for variable calcination. It indicates that the synthesized ZnO nano particles are not single crystals , rather are the aggregates of several singla crystals.

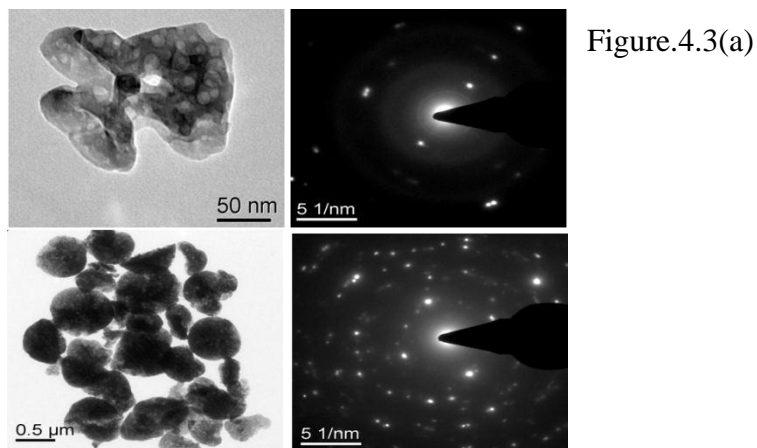


Figure.4.3(a) TEM images & SAED pattern of sample S2 calcined at 700°C at different magnification .

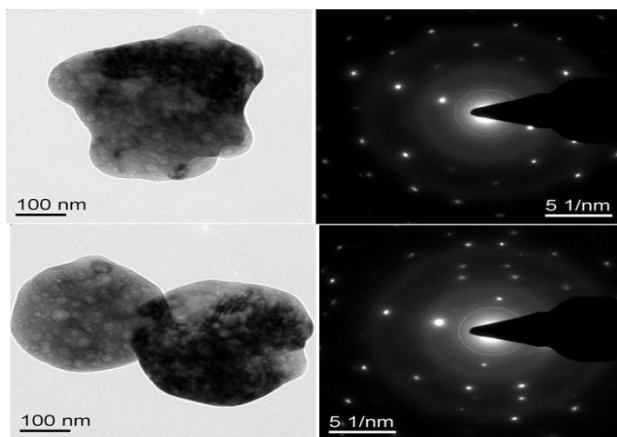


Figure. 4.3.(b) TEM images & SAED pattern of sample S3 calcined at 900°C.

4.4. Fourier Transform Infrared Spectroscopy (FTIR)

Figure.4.4. shows the FTIR spectrum of the ZnO nanoparticles synthesized by sol-gel method, which was acquired in the range of 400-4000 cm^{-1} . The band between the 450-500 cm^{-1} correlated to metal oxide bond (ZnO). From this FTIR we can also observe that increasing the annealing temperature sharpens of the characteristic peaks for metal oxide, suggesting that, the crystalline nature of ZnO increases on increasing the calcination temperature. The peaks in the range of 1400-1500 cm^{-1} corresponds to the C=O bonds. The adsorbed band at 1626 cm^{-1} is assigned O-H bending vibrations. The peak at 1319 cm^{-1} and 1530 cm^{-1} corresponds to C=O and O-H bending vibrations respectively diminishes gradually for sample annealed at higher temperature.

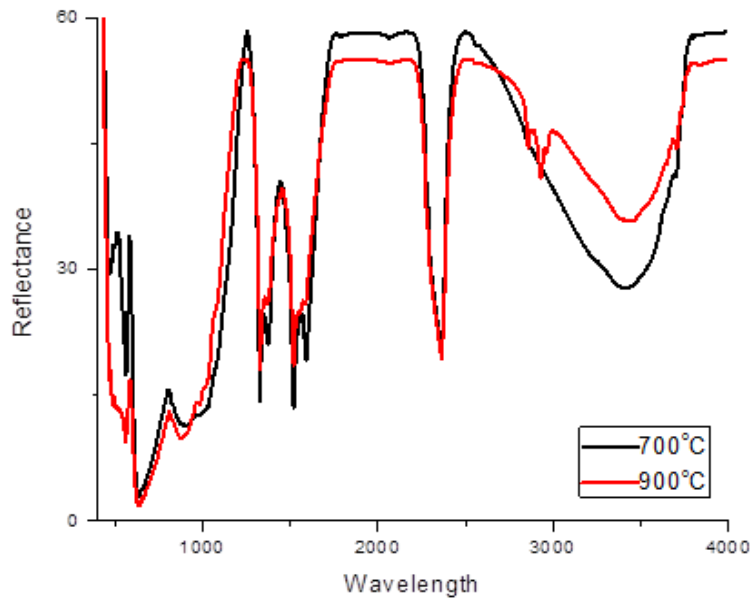


Figure.4.4. shows the FTIR peaks of samples S1 and S2 calcined at 700°C & 900°C respectively

4.5. UV- Visible spectroscopy

The band-gap energy (E_g) was determined based on numerical derivative of the optical absorption coefficient. The fundamental absorption method refers to band to band transitions by using Mott and Davis relation of Equation [52]. For photon energies just above fundamental edge, the absorption coefficient follows the standard relation.

$$\alpha = (\hbar\nu - E_g)^n A / \hbar\nu$$

where A is a constant related to the extent of the band tailing, $n = 1/2$ for allowed direct transition, $n=2$ for allowed indirect transition and E_g is the energy gap between the valence band and the conduction band. A graph of $((\alpha h\nu)^2$ versus $h\nu$) is as shown in Figure.4.6. by extrapolating the graph to X axis in order to calculated the band gap of the samples. The band gap is found to be 3.17eV & 3.18eV for the samples calcined at 700°C and 900°C for 4 hrs respectively. Thereby indicates that band gap remains almost same with increasing annealing temperature. Thus, from the value of band gap obtained 3.17eV agrees with the earlier reports [52] of the material.

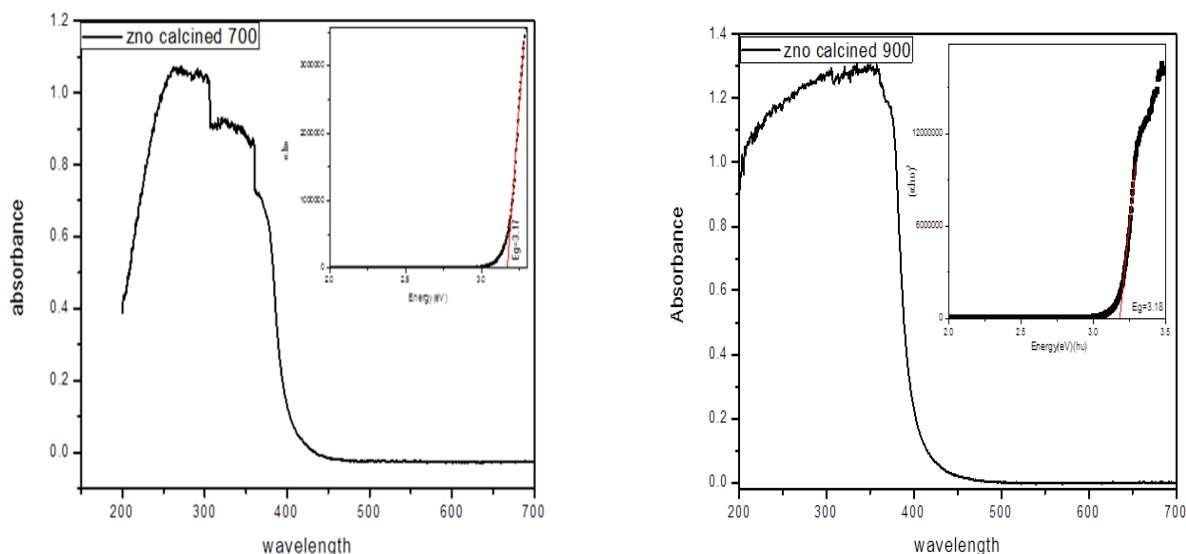


Figure.4.6. shows the UV report of samples calcined at 700°C & 900°C as well as band gap Obtained.

4.6.DSC & TGA

Figure.4.5. shows a combined plot of DSC and TGA. To determine the crystalline conditions, differential scanning calorimetry (DSC) and TGA of ZnO gel nanoparticles were carried out. The specimens were heated from room temperature to 1000°C with an increment of 10 °C/min in air. Notably, the TGA data plots the weight loss of the nanoparticles which shows that a small amount of weight loss has occurred around 100°C, there by indicating the

evaporation of water and/or moisture. As the DSC & TGA was carried out after calcination of the sample, so the DSC curve obtained shows multistate decomposition without forming any intermediates.

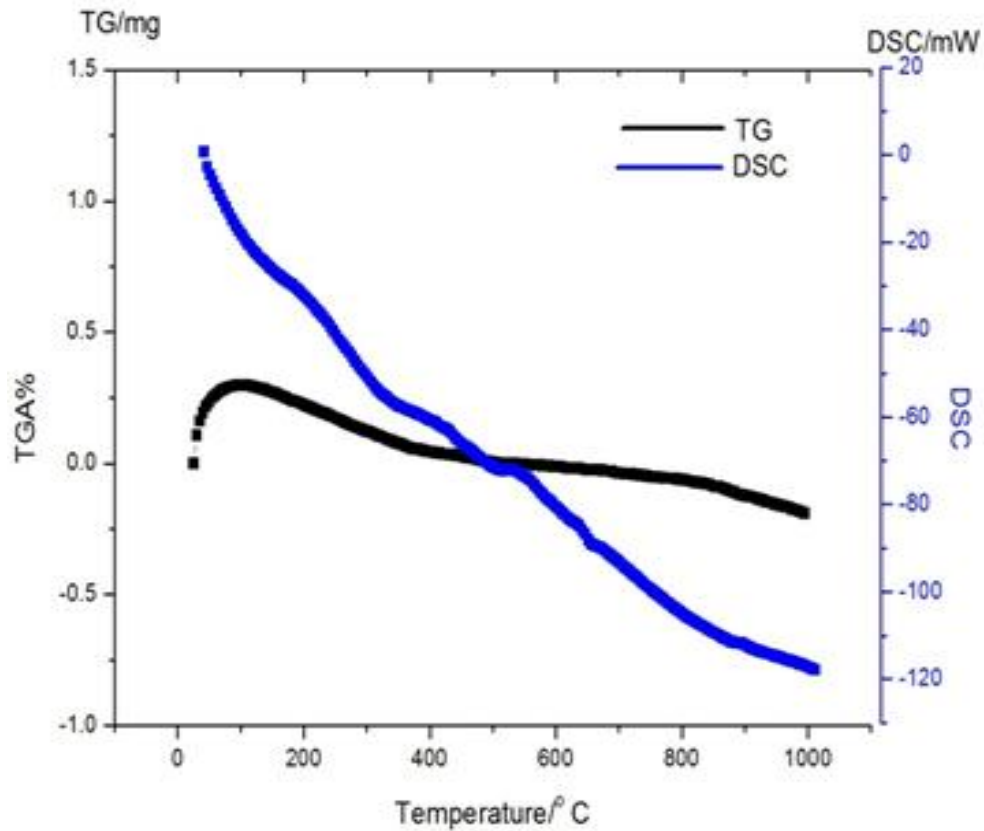


Figure.4.5. DSC & TG of the sample calcined at 700°C for 4 hr.

CHAPTER-5

CONCLUSION

Zinc oxide nanoparticles were synthesized through sol-gel method by considering different calcinations temperatures. The results of the XRD and TEM showed that the average particle size of ZnO particles increases with increasing calcinations temperature, and the SEM results showed that the formation of spherical shaped nanoparticles. Furthermore, the FTIR showed a broad absorption band related to Zn-O vibration band. The band gap of the zinc oxide nanoparticles was estimated from the UV-VIS absorption. It was observed that the band gap of the samples remains almost constant i.e (3.17eV) for different calcination temperature from 700°C to 900°C.

References

1. A.R. Hutson, Phys. Rev., 108(1957)222-230.
2. G. Heiland, E. Mollwo, F. Stockmann, Solid State Phys., 8(1959)193-196
3. J.R. Haynes, Phys. Rev. Lett., 17(1966)16.
4. Y.S. Park et al, Phys. Rev., 143(1966)2.
5. T. Damen, S.P.S Porto, B. Tell, Phys. Rev., 142(1966)2.
6. M. Matsuoka, J. J. App. Phys., 10(1971)736.
7. P.R. Emtage, J. App. Phys., 48(1977)4372-4384.
8. M. Inada, J. J. Phys., 17(1978)1-10.
9. F.S. Hickerne, J. App. Phys., 44(1973), 1061-1071.
10. S.K. Tiku, C.K. Lau, K.M. Lakin, App. Phys. Lett., 35(1980)318-320.
11. C. Eberspacher, A.L. Fahrenbruch, R.H. Bube, Thin Solid Films, 136(1986)1-10.
12. P.F. Carcia, R.S. McLean, M.H. Reily, G. Nunes, Jr. App. Phys. Lett., 82(2003), 7.
13. N.J. Ianno, L. McConville, N. Shaikh, S. Pittal, P.G. Snyder, Thin Sol. Films, 220(1992)92-99.
14. T.V. Butkhuji et al., J. Crys. Growth, 117(1992)366-369.
15. D. Vogel, P. Krüger and J. Pollmann, Phys. Rev., 52(1995)14316-1431.
16. Tammy P. Chou, Qifeng Zhang, Glen E. Fryxell, Guozhong Cao, Adv. Mater., 19(2007)2588–2592.
17. Seema Rani, Poonam Suri, P.K. Shishodia, R.M. Mehra, 92(2008)1639–1645.
18. <http://www.microscopemaster.com/nanotechnology.html>
19. <http://www.scientificamerican.com/article.cfm?id=nanotechnologysfuture>.
20. http://www.nanotechnologies.qc.ca/projects/ZnO/ZnO_nanostructures#more
21. <http://anyfreepapers.com/free-research-papers/nanotechnology-research-paper.html>
22. <http://en.wikipedia.org/wiki/Nanotechnology>
23. C. Jagadish and S. J. Pearton, “Zinc Oxide Bulk, Thin Films and Nanostructures Processing, Properties and Application” Elsevier (2006).
24. Z. L. Wang and Z. C. Kang, Plenum press, (1998)465.
25. Z.L. Wang, J. Phys. Condensed Matter, 16(2004)829.
26. K. H. Hellwege, O. Madelung, A. M. Hellege, 19(1987)119-595.
27. Z. L. Wang, J. Phys., Condens. Matter, 16(2004)829–858.
28. G.H. Lee, Y. Yamamoto, M. Kourogia, M. Ohtsua, Thin Solid Films, 386(2001)117 - 120.
29. B. K. Meyer, H. Alves, D. M. Hofmann, W. Kriegseis et al., Phys. Stat. Sol., 241(2004)231-260.
30. Tingting Ren, Holly R. Baker, Kristin M. Poduska, Thin Solid Films, 515(2007)7976–7983.
31. Pijus Kanti Samanta and Partha Roy Chaudhuri, Science of Advanced Mater., 3(2011)107-112.

32. Chang Shi Lao et al., *Nanoletters*, 6(2006)263-266.
33. S. K. Mohanta, D. C. Kim, B. H. Kong, H. K. Cho, W. Liu, and S. Tripathy, *Sci. Adv. Mater.*, 2(2010)64.
34. R Ding, J. Liu, J. Jiang, X. Ji, X. Li, F. Wu, and X. Huang, *Sci. Adv. Mater.*, 2(2010)396.
35. Z. L. Wang, *Mater. Sci. Eng.* 33(2009)64.
36. . Y. Ding and Z. L. Wang, *Micron.*, 40(2009)335.
37. . M. Wei¹, D. Zhi, and J. L. MacManus-Driscoll, *Nanotechnology*, 16(2005)1364.
38. J. Jie, G. Wang, X. Han, Q. Yu, Y. Liao, G. Li, and J. G. Hou, *Chem. Phys. Lett.* 387(2004),466.
39. J. Zhang, W. Yu, and L. Zhang, *Phys. Lett. A* 299(2002)276.
40. M. H. Huang, S. Mao, H. Feick, H. Yan, Y. Wu, H. Kind, E. Weber, R. Russo, and P. Yang, *Science*, 292(2001)1897.
41. P. X. Gao, Y. Ding, and Z. L. Wang, *Nano Lett.*, 9(2009)137.
42. B. Tang, H. Deng, Z. W. Shui, and Q. Zhang, *J. Nanosci. Nanotechnol.* 10(2010)1842.
43. M. Vafaei, M. SasaniGhamsari^{b,*}, *Materials Letters*, 61 (2007)3265–3268.
44. M. Veith, M. Haas, and V. Huch, *Chem. Mater.*, 17(2005)95-101.
45. Kang X. Ya, Wang TianDiao, Han Yin, Tao MinDe, *Mater. Research Bulletin*, 32(1997), 1165-1171.
46. Eric A. Meulenkamp, *J. Phys. Chem. B.*, 102(1998)5566-5572.
47. M. Risti et al., *Journal of Alloys and Compounds* , 397 (2005)L1–L4.
48. Rizwan Wahab, S.G. Ansari, Young-Soon Kim, Hyung-Kee Seo, Hyung-Shik Shin *Appl. Surf. Sci.*, 253 (2007)622–7626.
49. Yongfa Zhu, Li Zhang, Chong Gao, Lili , *J. Mater. Sci.*, 35 (2000)4049–4054.
50. http://serc.carleton.edu/research_education/geochemsheets/techniques/SEM.html
51. <http://www.scribd.com/doc/21053651/Electronic-spectroscopy-UV-Visible>
52. Mott, N.F. and Davis, E.A., Clarendon Press, Oxford (1971) .
53. http://en.wikipedia.org/wiki/Scanning_electron_microscope
54. http://en.wikipedia.org/wiki/Transmission_electron_microscopy
55. mmrc.caltech.edu/FTIR/FTIRintro.pdf
56. http://en.wikipedia.org/wiki/Fourier_transform_infrared_spectroscopy#Conceptual_introduction
57. http://en.wikipedia.org/wiki/Thermal_analysis.

